Chinese Chemical Letters 37 (2026) 112407

Contents lists available at ScienceDirect

Chinese Chemical Letters

journal homepage: www.elsevier.com/locate/cclet

Ultrasensitive upconversion nanoprobe-based biosensor for dual-modal detection of thrombin and hirudin

Xiaohui Liu[a], Ruoyu Ba[a], Fen Wan[a], Yang Liu[a], Feng Lu[c], Jing-Jing Zhang[b], Peidong Chen[a], Yi Zhang[a], Jun-Jie Zhu[b,*], Li Zhang[a,*], Fang-Fang Cheng[a,*]

[a] *Jiangsu Collaborative Innovation Center of Chinese Medicinal Resources Industrialization, National and Local Collaborative Engineering Center of Chinese Medicinal Resources Industrialization and Formulae Innovative Medicine, Jiangsu Key Laboratory for High Technology Research of TCM Formulae, Nanjing University of Chinese Medicine, Nanjing 210023, China*
[b] *State Key Laboratory of Analytical Chemistry for Life Science, School of Chemistry and Chemical Engineering, Nanjing University, Nanjing 210023, China*
[c] *State Key Laboratory for Organic Electronics and Information Displays and Institute of Advanced Materials IAM, Nanjing University of Posts and Telecommunications, Nanjing 210023, China*

ARTICLE INFO

Article history:
Received 28 May 2025
Revised 6 November 2025
Accepted 12 January 2026
Available online 12 January 2026

Keywords:
Thrombin
Hirudin
Dual-modal
Upconversion nanoprobe
Chinese medicine

ABSTRACT

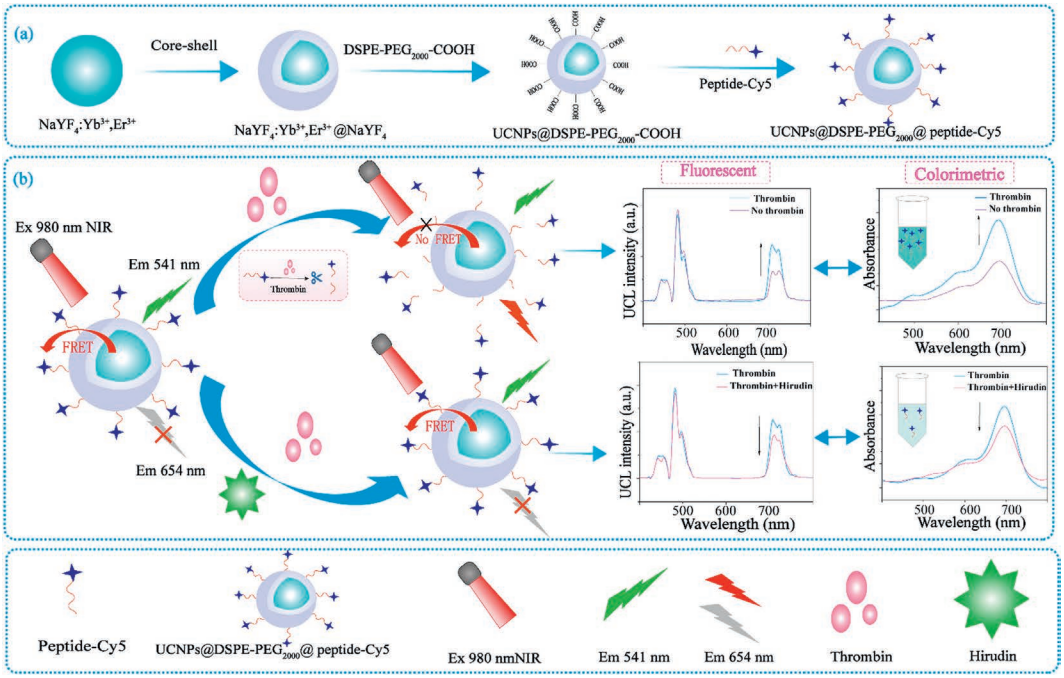
Thrombin can participate in many physiological and pathological processes so that its sensitive determination is important in diagnostic and pharmaceutical fields. The content of hirudin in leech is a key criterion for determining the quality of leech. In this work, a dual-modal biosensor was constructed based on fluorescence resonance energy transfer between UCNPs and Cy5 *via* a thrombin-responsive peptide as a linker. Thrombin cleaved the peptide and Cy5 released, leading to the fluorescence recovery of UCNPs at a specific wavelength, which enabled the successful ratiometric fluorescence detection of thrombin. Simultaneously, Cy5 in the supernatant allowed a colorimetric detection. Hirudin inhibited the activity of thrombin, causing the intensity reduction of the corresponding fluorescence and absorbance signals. The linear ranges of the fluorescence and colorimetric detection for thrombin were $10^{-9} \sim 10^{-4}$ U/mL with a detection limit of 1.15×10^{-10} U/mL and 0.0025–5 U/mL with a detection limit of 1.12×10^{-3} U/mL, respectively. The linear ranges of the fluorescence and colorimetric detection for hirudin were 10^{-8}–10^{-4} U/mL with a detection limit of 6.026×10^{-9} U/mL and 0.005–5 U/mL with a detection limit of 2.82×10^{-3} U/mL, respectively. This developed biosensor was further applied to the detection of anti-thrombin components in leech extract and the results showed that it had an excellent analytical performance, indicating this dual-modal biosensor provided a new specific and sensitive method for the detection of anti-thrombin components in practical sample, which is significant in quality evaluation of traditional Chinese medicine.
© 2026 Published by Elsevier B.V. on behalf of Chinese Chemical Society and Institute of Materia Medica, Chinese Academy of Medical Sciences.

Thrombin is a serine protease involved in many physiological and pathological activities such as blood coagulation, cardiovascular disease, liver disease, Alzheimer's disease, leukemia, and other blood-related diseases [1]. The activity of thrombin is a truer representation of its biological function and a better indication of the disease state [2]. Therefore, the detection of thrombin activity is very essential. Recently, a number of methods have been developed for thrombin activity detection, including fluorescence [3,4], colorimetric [5], surface enhanced Raman scattering [6], electrochemical [7] and electrochemiluminescence [8,9]. To enhance the accuracy and versatility, integration technology was usually used [10,11]. For example, Bi *et al.* [12] developed a dual-channel assay for thrombin based on photoelectrochemical and differential pulse voltammetry methods. Ali *et al.* [13] developed a dual-channel assay for thrombin based on colorimetric and fluorescence methods.

Hirudin, extracted from *Hirudo medicinalis*, is a natural and effective inhibitor of thrombin, which has good anticoagulant and antithrombotic effects. They can be used as therapeutic ingredients for cardiovascular disease, while they can be considered toxic peptides with a risk of bleeding [14]. The activity of anti-thrombin components in leech serves as a key criterion for determining the quality of leech. In the Chinese Pharmacopoeia, hirudin activity is assessed by thrombin inhibition assay that thrombin is added into leech extract until fibrin formation is observed with the naked eye [15]. However, this method is highly subjective and cannot be accurately quantitatively analyzed. High performance liquid chromatography is applied to quantitatively detect hirudin, but the purification processes is complicated [16]. Therefore, it is significant

* Corresponding authors.
E-mail addresses: jjzhu@nju.edu.cn (J.-J. Zhu), zhangli@njucm.edu.cn (L. Zhang), ffcheng@njucm.edu.cn (F.-F. Cheng).

https://doi.org/10.1016/j.cclet.2026.112407
1001-8417/© 2026 Published by Elsevier B.V. on behalf of Chinese Chemical Society and Institute of Materia Medica, Chinese Academy of Medical Sciences.



Scheme 1. Schematic representation of a UCNPs-based FRET biosensor for the detection of thrombin and hirudin *in vitro*.

to develop a sensitive and simple method for hirudin detection. Considering that hirudin is a powerful active inhibitor of thrombin, thrombin is usually used as a recognizer of hirudin to improve specificity [17]. The main issue to be considered in hirudin detection is how to enhance the sensitivity.

Upconversion nanoparticles (UCNPs) is a special type of lanthanide-doped nanoparticles capable of emitting multicolored ultraviolet and visible light upon excitation of near-infrared (NIR) light [18]. UCNPs is widely used to construct highly sensitive biosensors due to their unique properties including narrow emission peaks, deep penetration depth in biological tissues, high photostability, low toxicity, low autofluorescence background, and resistance to photobleaching, *etc.* [19,20]. Studies have shown that UCNPs is an effective fluorescence resonance energy transfer (FRET) donor for various bioanalytical and biomedical applications [21]. UCNPs-based FRET probes have been widely used for the detection of various analytes such as DNA [22], metal ions [23,24], biomolecules [25,26] and enzymes [27]. In addition, UCNPs have the nature of multi-wavelength emission so that one wavelength can be set as the reference wavelength and the other wavelength as the detection wavelength to design the ratiometric fluorescent probes. Compared to single-signal intensity-based "turn-on/off" fluorescent probes, ratiometric fluorescent probes can eliminate signal interference from the test environment, including radiation light fluctuation and probe concentration, thereby enhancing detection accuracy and sensitivity [28,29].

Herein, a fluorescence and colorimetric dual-modal biosensor was developed for thrombin and hirudin detection by conjugating a Cy5 modified thrombin-responsive peptide (peptide-Cy5) with carboxylated UCNPs (UCNPs@DSPE-PEG_{2000}–COOH). As shown in Scheme 1, this dual-modal biosensor was constructed using UCNPs as an energy donor and Cy5 as an energy acceptor. Under the excitation of 980 nm near-infrared laser, UCNPs showed dual UCL emission bands at 541 nm (green) and 654 nm (red), respectively. The absorption band of Cy5 was centred at 650 nm, which overlapped well with the UCL emission of UCNPs at 654 nm, implying that the FRET process could occur between UCNPs and Cy5. In the absence of thrombin, the red UCL fluorescence signal of UCNPs was quenched by Cy5. When thrombin was present, thrombin cleaved the substrate peptide and Cy5 was released, resulting in the recovery of the UCL fluorescence signal of UCNPs at 654 nm. The recovery ratio of UCL emission at 654 nm was dependent on thrombin activity. In addition, the UV–vis absorbance of the supernatant increased with the release of Cy5, thus allowing the detection of a colorimetric signal. Hirudin could inhibit thrombin activity, leading to a decrease in thrombin cleavage efficiency and a corresponding decrease in fluorescence and colorimetric signal. Thus, the detection of hirudin could be achieved indirectly. The method was also successfully applied to the detection of anti-thrombin components in leech extract. During the detection process, the UCL signal of the UCNPs at 541 nm could be used as an internal reference for ratiometric sensing since it was not affected before and after Cy5 release.

The synthesized $NaYF_4$:Yb^{3+}, Er^{3+}, $NaYF_4$:Yb^{3+}, Er^{3+}@ $NaYF_4$, UCNPs@DSPE-PEG_{2000}–COOH and UCNPs@DSPE-PEG_{2000}@ peptide-Cy5 were characterized using TEM (Figs. 1a-d). $NaYF_4$:Yb^{3+}, Er^{3+} exhibited a uniform hexagonal phase structure due to anisotropic growth in the selected solvent, with an average particle size of 33.55±0.85 nm (Fig. 1e). A layer of $NaYF_4$ shell was modified on the surface of $NaYF_4$:Yb^{3+}, Er^{3+} to form a core-shell structure of $NaYF_4$:Yb^{3+}, Er^{3+} @ $NaYF_4$. Due to the heteroepitaxial growth of the shell layer, the original growth kinetics were altered by lattice strain and surface energy control, resulting in the formation of a square structure. The average particle size of $NaYF_4$:Yb^{3+}, Er^{3+} @$NaYF_4$ was 36.27 ± 0.75 nm (Fig. 1f), indicating that the thickness of the shell layer of $NaYF_4$ was about 1.36 nm. After modification of DSPE-PEG_{2000}–COOH (Fig. 1g) and peptide-Cy5 (Fig. 1h), the average particle size of UCNPs@DSPE-PEG_{2000}@peptide-Cy5 increased to 43.11±0.71 nm, indicating their successful modification.

Fluorescence spectroscopy of $NaYF_4$:Yb^{3+}, Er^{3+}, $NaYF_4$:Yb^{3+}, Er^{3+}@$NaYF_4$ and UCNPs@DSPE-PEG_{2000}–COOH were detected (Fig. 1i). The results showed that the core-shell structure significantly enhanced the UCL intensity compared to the core structure, attributed to the fact that the presence of the shell could greatly enhance the luminescence of UCNPs and reduce the surface fluorescence quenching [30,31]. After mod-

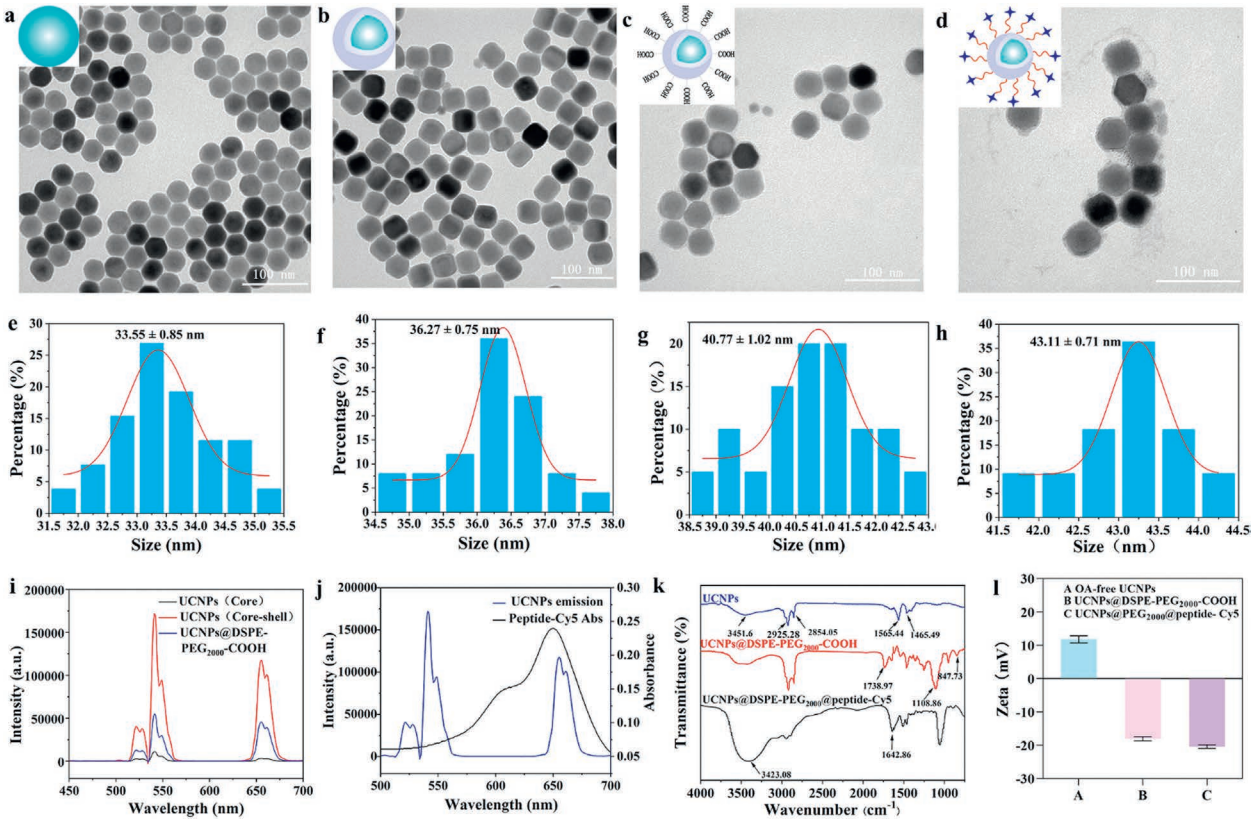


Fig. 1. TEM micrographs of (a) $NaYF_4$:Yb^{3+}, Er^{3+}, (b) $NaYF_4$:Yb^{3+}, Er^{3+}@$NaYF_4$, (c) UCNPs@DSPE-PEG_{2000}−COOH and (d) UCNPs@DSPE-PEG_{2000}@peptide-Cy5, respectively. The scale bars are 100 nm. (e-h) The corresponding size distribution of UCNPs of (a-d). (i) Fluorescence profiles of $NaYF_4$:Yb^{3+}, Er^{3+} (UCNPs core); $NaYF_4$:Yb^{3+}, Er^{3+}@$NaYF_4$ (UCNPs core-shell) and UCNPs@DSPE-PEG_{2000}−COOH. (j) The emission spectra of UCNPs and absorption spectra of Cy5. (k) FT-IR spectra of $NaYF_4$:Yb^{3+}, Er^{3+}@$NaYF_4$ (UCNPs), UCNPs@DSPE-PEG_{2000}−COOH and UCNPs@DSPE-PEG_{2000}@peptide-Cy5. (l) Zeta potentials of $NaYF_4$:Yb^{3+}, Er^{3+}@$NaYF_4$ (OA-free UCNPs), UCNPs@DSPE-PEG_{2000}−COOH and UCNPs@DSPE-PEG_{2000}@peptide-Cy5. Error bars represented the standard deviation of three independent measurements ($n = 3$).

ification of DSPE-PEG_{2000}−COOH, and the UCL intensity of UCNPs@DSPE-PEG_{2000}−COOH was significantly reduced compared to $NaYF_4$:Yb^{3+},Er^{3+}@$NaYF_4$ due to the luminescence quenching effect in aqueous environment [32]. In Fig. 1j, the absorption band of Cy5 centered at 650 nm overlapped well with the UCL emission of UCNPs centered at 654 nm. It was demonstrated that Cy5 could quench the 654 nm fluorescence of UCNPs well. Fourier transform infrared spectroscopy (FT-IR) was also performed to characterize the prepared UCNPs (Fig. 1k). The UCNPs showed significant absorption peaks at 2924 cm^{-1} and 2856 cm^{-1}, which could be attributed to the asymmetric and symmetric stretching vibrations of the methylene group (-CH_2-) on the free chain of OA. The peaks at 1557 cm^{-1} and 1465 cm^{-1} were attributed to the asymmetric and symmetric stretching vibrations of the carboxylic acid (-COO-), respectively. After DSPE-PEG_{2000}−COOH functionalization, the new peak at 844 cm^{-1} was attributed to the in-plane bending vibration of -CH_2−CH_2−O-, while the two new peaks at 1738 cm^{-1} and 1108 cm^{-1} were attributed to the stretching vibration of carboxylic ester and ether bond of the PEG chain, respectively, confirming the successful modification of DSPE-PEG_{2000}−COOH. After linking peptide-Cy5, the peak 3423 cm^{-1} was attributed to the stretching vibration of -N-H- in the amide, indicating the successful covalent modification of peptide-Cy5. In Fig. 1l, due to the negative charge of DSPE-PEG_{2000}−COOH, the zeta potential value of UCNPs after modification changed from positive to negative charge. Due to the negative charge of petide-Cy5 in solution with the pH of 7.4, the zeta potential decreased from −18.06 mV to −20.4 mV, indicating that petide-Cy5 was covalently modified onto UCNPs@DSPE-PEG_{2000}−COOH.

In order to obtain the best detection performance of the probes, the experimental conditions were optimized. The results demonstrated that the optimal added amount of DSPE-PEG_{2000}−COOH was determined to be 1.25 mg and the optimal ratio of peptide-Cy5 to UCNP@DSPE-PEG_{2000}−COOH was 0.02 (Fig. S1 in Supporting information). Under optimized experimental conditions, the probes were used to detect different concentrations of thrombin. Thrombin could specifically cleave the probe's responsive peptide site of Peptide-Cy5 (sequence: GGLVPRGSC(Cy5)) between R and G. Upon cleavage of the peptide chain by thrombin, the Cy5-containing peptide fragment was released so that FRET action was disrupted, and fluorescence at 654 nm was restored. The results were shown in Fig. 2a, where the UCL intensity of UCNPs at 654 nm increased proportionally with the increase of thrombin concentration, while the UCL intensity at 541 nm showed no significant change to the concentrations of thrombin. This was due to the selective cleavage of the substrate peptide by thrombin and the release of the quencher Cy5, which in turn destroyed FRET, allowing the recovery of UCL fluorescence at 654 nm. Under 980 nm laser excitation. The fluorescence intensity ratio ($I_{654\ nm}/I_{541\ nm}$) gradually increased with the increase of thrombin concentration. When the thrombin concentration increased to 1×10^{-4} U/mL, the peptide probe was gradually depleted and the fluorescence intensity ratio began to reach a saturated state (Fig. S2 in Supporting information). The fluorescence intensity ratio ($I_{654\ nm}/I_{541\ nm}$) showed a good linear relationship with the logarithm of thrombin concentrations in the range of $1 \times 10^{-9} \sim 1 \times 10^{-4}$ U/mL (Fig. 2b). The linear regression equation was $y = 3.184 \lg C_{Thrombin} + 69.28$ with a correlation coefficient (R^2) of 0.9907. Referring to the calculation method of Zhang

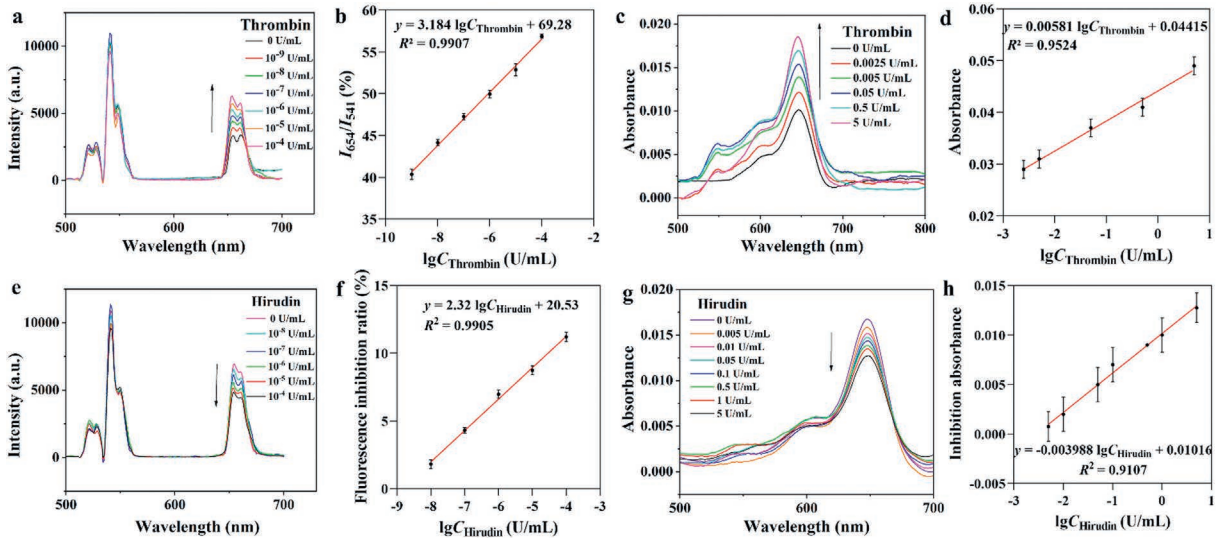


Fig. 2. (a) UCL spectra of the probes after adding different concentrations of thrombin. (b) Linear relationship between the ratio of UCL intensities at 654 nm and 541 nm and the logarithm of thrombin concentrations in the range of 1×10^{-9} U/mL to 10^{-4} U/mL ($n = 3$). (c) UV absorption spectra of the supernatants after the probes incubating with different concentrations of thrombin. (d) Linear relationship between UV absorbance at 650 nm and the logarithm of thrombin concentrations in the range of 0.0025 U/mL to 5 U/mL ($n = 3$). (e) UCL spectra of the probes after adding different concentrations of hirudin. (f) Linear relationship between the fluorescence inhibition ratio and the logarithm of hirudin concentration in the range of 1×10^{-8} U/mL to 1×10^{-4} U/mL ($n = 3$). (g) UV absorption spectra of the supernatant after adding different concentrations of hirudin. (h) Linear relationship between UV inhibition absorbance at 650 nm and the logarithm of hirudin concentrations in the range of 0.005 U/mL to 5 U/mL ($n = 3$).

et al. [22], the limit of detection (LOD) was 1.15×10^{-10} U/mL (S/N = 3), which was lower than most of the nanoprobes used in the literature for thrombin detection (Table S1 in Supporting information). With the increasing thrombin concentration, Cy5 was continuously released and the absorbance of the supernatant was measured (Fig. 2c). The absorbance showed a good linear relationship with the logarithm of thrombin concentrations in the range of 0.0025–5 U/mL (Fig. 2d). The linear regression equation was $y = 0.00581 \lg C_{\text{Thrombin}} + 0.04415$ with a correlation coefficient (R^2) of 0.9524 and a limit of detection (LOD) of 1.12×10^{-3} U/mL. In addition, the probes were incubated with other enzymes and mixed enzyme, the results demonstrated that this biosensor exhibited excellent specificity and anti-interference properties (Fig. S3 in Supporting information).

The detection and screening of protease inhibitors play an important role in the development of new drugs. Hirudin, one of the most potent thrombin inhibitors, was used as a model to test the potential extension of our method to thrombin inhibitor detection. It was found that the UCL intensities of UCNPs at 654 nm decreased with increasing hirudin concentration at fixed concentrations of thrombin (100 μU/mL) and UCNPs@DSPE-PEG_{2000}@peptide-Cy5 probes, whereas the UCL intensities at 541 nm showed no significant changes (Fig. 2e). This was likely that hirudin inhibited the activity of thrombin, leading to a decrease in the cleaving efficiency of thrombin to the substrate and a corresponding decrease in the fluorescence signal. The fluorescence inhibition ratio of thrombin was calculated by the following formula: Fluorescence inhibition ratio = $R_0 - R$ (where R_0 is the fluorescence intensity I_{654}/I_{541} ratio in the absence of hirudin and R is the fluorescence intensity I_{654}/I_{541} ratio in the presence of hirudin). The fluorescence inhibition ratio increased with the increasing hirudin concentration and showed a good linear relationship with the logarithm of hirudin concentration in the range of $1 \times 10^{-8} \sim 1 \times 10^{-4}$ U/mL (Fig. 2f). The linear regression equation was $y = 2.32 \lg C_{\text{Hirudin}} + 20.53$ with a correlation coefficient (R^2) of 0.9905. The limit of detection (LOD) was 6.026×10^{-9} U/mL, which was lower than most of the methods reported in the literatures (Table S2 in Supporting information). In addition, the absorbance of the supernatant decreased continuously with increasing hirudin concentrations because of the inhibition of thrombin activity to the cleavage of the substrate peptide that the amount of the released Cy5 decreased (Fig. 2g). Inhibition absorbance = $A_0 - A$ (where A_0 was the absorbance in the absence of hirudin and A was the absorbance in the presence of hirudin). The inhibition absorbance showed a good linear relationship with the logarithm of hirudin concentration in the range of 0.005–5 U/mL (Fig. 2h). The linear regression equation was $y = 0.003988 \lg C_{\text{Hirudin}} + 0.01016$ with a correlation coefficient (R^2) of 0.9107 and a LOD of 2.82×10^{-3} U/mL.

To validate the selectivity of our method for hirudin, the other two thrombin inhibitors, bivalirudin and argatroban, were selected for comparative analysis. Bivalirudin shows structural similarity to hirudin. Fig. S4 (Supporting information) presented the dose-response curves for both drugs. The results indicated that both drugs exhibited significant inhibitory effects on thrombin, but there was no linear relationship. In contrast, Fig. 2f showed that hirudin exhibited a clear linear range. This may be due to the fact that the inhibitor reaction to thrombin of bivalirudin and argatroban were reversible, whereas the reaction of hirudin was irreversible. This demonstrated that hirudin exhibited good selectivity.

In order to investigate the accuracy and precision of the method for the detection of hirudin in leech extract, the spiked recovery test was used for validation. The results were shown in Table S3 (Supporting information). The spiked recovery rates of sample 1, sample 2 and sample 3 were 104.97 %, 96.16 % and 95.5 % with the corresponding relative standard deviations (RSD) of 2.36 %, 1.91 % and 1.61 %, respectively. This test indicated that the established method had the high accuracy and precision.

To examine the practicality of the method, the biosensor was applied to the detection of anti-thrombin components in the leech extract. The results were shown in Fig. 3. The fluorescence inhibition ratio (blue line) showed a good linear relationship with the logarithm of the concentration of the leech extract in the range of 1×10^{-8} to 1×10^{-4} mg/mL. The linear regression equation was $y = 2.3711 \lg C_{\text{Leech}} + 20.33$ with a correlation coefficient (R^2) of 0.9153 and a LOD of 4.9×10^{-9} mg/mL. Also, based on the linear relationship between the fluorescence inhibition ratio and the logarithm of the hirudin concentration in Fig. 2f, the concentration of hirudin were calculated which represented the to-

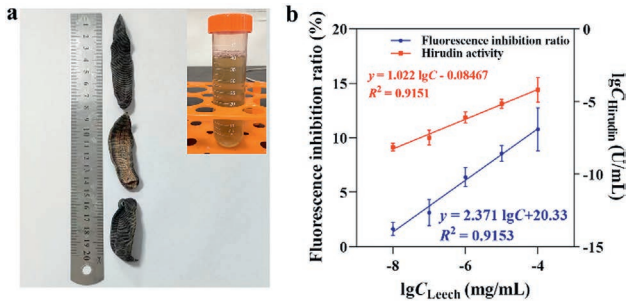


Fig. 3. (a) The images of leech and its extract solution. (b) Blue line indicated the relationship between the fluorescence inhibition ratio and the logarithm of leech extract concentration. Red line indicated the relationship between the logarithm of the concentrations of hirudin and the logarithm of the concentrations of leech extract ($n = 3$). Note: $C_{hirudin}$ is defined as the concentration of anti-thrombin components equivalent to the concentration of hirudin.

tal concentration of anti-thrombin components. As Fig. 3b (red line) showed, the logarithm of the concentration of hirudin in the leech extract showed a good linear relationship with the logarithm of the concentrations of the leech extract in the range of 1×10^{-8} to 1×10^{-4} mg/mL. The linear regression equation was $\lg C_{Hirudin} = 1.0221 \lg C_{Leech} - 0.08467$ with a correlation coefficient (R^2) of 0.9151.

In summary, we constructed a dual-modal biosensor consisting of UCNPs as an energy donor and a Cy5-modified peptide for the detection of thrombin and hirudin. This biosensor can simultaneously generate accurate and sensitive fluorescence and absorbance signals for thrombin activity detection, thereby indirectly enabling hirudin's antithrombin activity detection, which has good stability, excellent specificity and low interference. This dual-modal fluorescence and colorimetric assay can complement each other. The fluorescence assay is extremely sensitive and is used for high-sensitivity quantification, with particular advantages in the complex biological sample hirudin. The colorimetric assay has a wide dynamic range and is suitable for medium to high concentrations of drugs, where changes in concentration can be determined by the naked eye or a simple spectrometer, and can be used for rapid visual screening. The combination of the two methods avoids the concentration limitation of a single method, achieves complementary sensitivity and detection range, and improves the anti-interference ability. It makes the method rapid, accurate and applicable. Moreover, in fluorescence assays, the ratiometric fluorescence method was introduced that the fluorescence intensity at 541 nm was used as an internal reference, which would greatly reduce the background interference and improve the accuracy of the analysis. This biosensor was further successfully carried out for the practical fluorescence detection of hirudin in the leech extract with a good linear range and recovery rate because their unique emission light can effectively avoid the color interference caused by the leech extract. Overall, this dual-modal biosensor provides a new platform for the detection of hirudin-like components in the leech and a new vision for the accurate determination of the active components in traditional Chinese medicine.

CRediT authorship contribution statement

Xiaohui Liu: Writing – review & editing, Writing – original draft, Methodology, Investigation, Data curation, Conceptualization. **Ruoyu Ba:** Writing – original draft, Methodology, Investigation. **Fen Wan:** Writing – original draft, Investigation. **Yang Liu:** Writing – original draft, Methodology, Investigation. **Feng Lu:** Resources, Methodology. **Jing-Jing Zhang:** Resources, Methodology. **Peidong Chen:** Validation, Funding acquisition. **Yi Zhang:** Writing – review & editing, Validation. **Jun-Jie Zhu:** Writing – review & editing, Supervision. **Li Zhang:** Supervision, Funding acquisition. **Fang-Fang Cheng:** Writing – review & editing, Supervision, Methodology, Funding acquisition, Conceptualization.

Declaration of competing interest

The authors declare that they have no known competing financial interests or personal relationships that could have appeared to influence the work reported in this paper.

Acknowledgments

The authors are thankful to the National Natural Science Foundation of China (Nos. 82374039, 82374037, and 21705081), the Natural Science Foundation of Jiangsu Province (No. BK20231258), Project funded by Jiangsu Administration of Traditional Chinese Medicine (No. MS2021005), Scientific Research Cultivation Project of First-class Discipline of Traditional Chinese Medicine in Nanjing University of Chinese Medicine (No. ZYXPY2024-003).

Supplementary materials

Supplementary material associated with this article can be found, in the online version, at doi:10.1016/j.cclet.2026.112407.

References

[1] X. Liu, R. Ba, W. Wang, et al., TrAC-Trend. Anal. Chem. 175 (2024) 117734.
[2] A. Megia-Fernandez, B. Mills, C. Michels, et al., Org. Biomol. Chem. 15 (2017) 4344–4350.
[3] X. Jin, X. Liu, X. Zhu, et al., Anal. Methods 8 (2016) 3691–3697.
[4] L. Zhao, F. Ahmed, H. Xiong, Chin. Chem. Lett. 33 (2022) 4243–4247.
[5] Y. Muto, T. Zako, Anal. Sci. 38 (2022) 3–7.
[6] P. Anantha, P. Raj, P. Zheng, et al., Sensor. Actuat. B: Chem. 423 (2025) 136811.
[7] Q. Hu, Y. Bao, S. Gan, et al., Anal. Chem. 92 (2020) 3470–3476.
[8] J. Zhang, D. Xu, Z. Deng, et al., Talanta 267 (2024) 125267.
[9] D. Xu, Y. Wang, J. Zhang, et al., Microchem. J. 207 (2024) 112147.
[10] Y. Sun, X. Zhu, H. Liu, et al., ACS Appl. Mater. Interfaces 12 (2020) 5569–5577.
[11] J. Liu, J. Zhang, C. Zhou, et al., Microchim. Acta 190 (2023) 444.
[12] S. Bi, C. Chai, H. He, et al., Biosens. Bioelectron. 272 (2025) 117132.
[13] G.K. Ali, K.M. Omer, ACS Omega 7 (2022) 36804–36810.
[14] X. Cao, Y. Luo, X. Liu, et al., Talanta 267 (2024) 125244.
[15] Chinese Pharmacopoeia Commission, Pharmacopoeia of People's Republic of China Part 1, Beijing, 2025, pp. 95.
[16] Q. Huang, Q. Gao, X. Chai, et al., J. Chromatogr. B Analyt. Technol. Biomed. Life Sci. 1151 (2020) 204–213.
[17] Y. Liu, J. Yang, J. Wang, et al., Blood Coagul. Fibrin. 26 (2015) 823–826.
[18] K. Malhotra, D. Hrovat, B. Kumar, et al., ACS Appl. Mater. Interfaces 15 (2023) 2499–2528.
[19] Y. Zhan, R. Zhang, Y. Guo, et al., J. Mater. Chem. B 11 (2023) 755–771.
[20] P. Liu, S. Zhang, T. Zhang, et al., Chin. Chem. Lett. 37 (2026) 110966.
[21] X. Zhou, H. Geng, P. Shi, et al., Biosens. Bioelectron. 247 (2024) 115916.
[22] Y. Zhang, D. Luo, Y. Zhang, et al., Chem. Eng. J. 454 (2023) 140489.
[23] L. Huang, F. Chen, X. Zong, et al., Talanta 227 (2021) 122156.
[24] Q.Q. Wang, R. Hu, Z.Q. Fang, et al., Chin. Chem. Lett. 33 (2022) 3782–3786.
[25] Y. Qin, K. Chen, Z. Wei, et al., Talanta 298 (2026) 129015.
[26] Y. Chen, T. Zhang, X. Gao, et al., Chin. Chem. Lett. 28 (2017) 1983–1986.
[27] X. Li, M. Zhang, H. Zhang, et al., Microchim. Acta 190 (2023) 181.
[28] C. Liu, Y. Lin, Z. Chen, et al., J. Agric. Food Chem. 72 (2024) 23580–23591.
[29] X. Chen, Q. Yang, X. Lv, et al., Coord. Chem. Rev. 516 (2024) 215970.
[30] F. Wang, J. Wang, X. Liu, Angew. Chem. Int. Ed. 49 (2010) 7456–7460.
[31] H. Xu, M. Jia, Z. Wang, et al., ACS Appl. Mater. Interfaces 13 (2021) 61506–61517.
[32] R. Arppe, I. Hyppänen, N. Perälä, et al., Nanoscale 7 (2015) 11746–11757.